

Development of A Grain Defects Resistant Ni-Based Single Crystal Superalloy YH61

Hideki TAMAKI¹, Akira OKAYAMA¹, Akira YOSHINARI¹
Kagehiro KAGEYAMA², Koji SATO² and Toshihiro OHNO²

¹Hitachi Research Lab., Hitachi, Ltd.

MD#840 7-1-1 Omika, Hitachi, Ibaraki 319-1292, JAPAN

Phone: +81-294-27-5028, FAX: +81-293-27-5059, E-mail: hidekit@hrl.hitachi.co.jp

²Metallurgical Research Lab., Hitachi Metals, Ltd.

ABSTRACT

When single crystal (SC) castings are adopted for industrial gas turbine's (IGT's) components, some degree of grain defects should be permitted to increase casting yield and reduce cost of the castings. In this paper, a new SC superalloy YH61 is proposed to solve the problem of grain defects which are present in SC buckets or vanes of IGTs. First, the effects of solution heat treatment on various properties of the SC with and without grain defects were evaluated. Increasing the solution-heat-treated area was found to have a positive effect on the strength of a defect-free SC but harmful for the strength across a grain boundary. The solution heat treatment condition for YH61 was determined after considering compatibility for properties of both the defect-free SC and the SC with grain defects. The solution heat treatment was also found to improve hot corrosion resistance of the alloy. Secondly, more detailed creep and hot corrosion tests were performed for YH61 solution-heat-treated by one of the above-examined conditions. YH61 showed higher creep strength than that of a second-generation directionally solidified (DS) superalloy although Re content of YH61 is about half as much as that of second-generation DS superalloys. Hot corrosion resistance of YH61 was superior to that of a second-generation DS superalloy under the whole experimental temperature range and to that of a 14% chromium containing conventional cast (CC) superalloy, which is currently used in some IGTs, when the test temperature was 1000°C.

INTRODUCTION

Application of SC buckets and vanes in aero-engines has significantly improved the engine performance. In the field of IGTs, application of SC components is necessary for improving the efficiency of IGTs due to increases in gas-firing temperature. Although this demand is common to all IGT manufacturers, DS buckets and vanes are still the mainstream technology for IGTs especially in the case of heavy-duty machines. As a result of considerable efforts for adopting SC components for IGTs (Cybulsky and Bryant, 1993), three IGT manufacturers have announced that they have introduced SC buckets or vanes into their machineries (Barker, 1995, Kiesow and Mukherjee, 1997 and Farmer, 2002).

The main reason why SC components have not been widely adopted for IGTs is the casting problems of the SC for IGT. Grain

defects such as low angle grain boundaries (LAB), high angle grain boundaries (HAB) and recrystallization tend to occur in IGT buckets or vanes, since their sizes are larger and their shapes are more complicated than those of the aero-engines' components. Because of these reasons, the casting yield of the SC for IGT is significantly lower and their cost is higher than the DS components. If the resistance of SC superalloys to LAB or HAB is increased, higher yields and lower costs can be realized for SC buckets and vanes in IGT. In order to meet these demands, a new SC superalloy, YH61 (Table 1) has been developed (Tamaki et al., 1998) and was found to show similar creep-rupture strength to a second-generation SC superalloy under certain conditions although YH61 contains higher levels of grain boundary strengthening elements (Tamaki et al., 2000). The highlights of its chemistry is summarized below:

- (1) Higher amounts of refractory elements such as Ta, W and Re are added in order to realize a similar level of creep-rupture strength as the second-generation SC superalloys without full solution
- (2) A higher content of boron compared to conventional DS alloys is used to keep an adequate level of boron at grain boundaries after solution heat treatment.

Table 1 Nominal Composition of YH61, mass%.

Cr	Co	W	Re	Mo	Ta	Nb	Al	Hf	C	B	Ni
7.2	1.0	8.8	1.4	0.9	8.8	0.8	5.0	0.25	0.07	0.02	Balance

It was pointed out by Jackson et al. (1977) and has been generally accepted that higher creep-rupture strengths along the solidification direction of SC and DS can be achieved by increasing the volume percent of fine γ' . Higher solution heat treatment temperatures are also known to increase the volume percent of fine γ' . For these reasons, solution heat treatment temperatures close to the incipient melting points have been adopted for conventional SC superalloys. Because such higher solution heat treatment temperatures can be achieved by removing grain boundary strengthening elements such as boron, hafnium and zirconium from the alloys, the conventional SC alloys can contain a limited range of LAB. Ross and O'Hara (1996) have reported a unique SC superalloy that has moderate LAB strength but higher grain boundary strength than this alloy is thought to be required for IGT.

For alloys with grain boundary strengthening elements, Cetel and Duhl (1992) pointed out that the creep-ductility for DS in the

transverse direction decreases with increasing volume percent of fine γ' . This increase was also found to decrease the creep-rupture life of DS in the transverse direction even in an alloy which contains grain boundary strengthening elements (Tamaki et al., 1998). Especially, the higher volume percent causes a significant decrease in the creep-rupture life of DS in the transverse direction. Thus, for achieving higher strength of LAB and HAB, both the addition of the grain boundary strengthening elements and optimizing solution heat treatment conditions seem to be necessary. This paper discusses optimization of the solution heat treatment condition for SC superalloys with grain defects.

When one new superalloy is adopted for IGTs, it should be required to obtain long-term creep data up to more than 10,000 hours of rupture life. This is generally longer than that required for aero-engines while main test temperatures are lower. Hot corrosion resistance is also major concern for IGTs, while oxidation resistance is regarded as more important in aero-engines' application. In case of IGTs, it should be noted that IGTs may be operated by various kinds of fuels such as heavy oil or residual oil which contains higher amount of sulfur than jet fuel. This paper discusses long-term creep properties of YH61 and hot corrosion resistance of the alloy to confirm applicability of the alloy to IGTs.

EXPERIMENTAL PROCEDURE

Seven 150 kg - master alloys and two 1.5 ton - master alloys of YH61 were prepared for this study. SC bars ($\phi 15 \times 165$ mm), DS slabs ($100 \times 15 \times 250$ mm) and bi-crystalline slabs described in Figure 1 were cast from the master alloys by a mold withdrawal method.

The conditions of the multistep solution heat treatment adopted for this alloy are listed in Table 2. The aging condition for all specimens was $1080^\circ\text{C}/4\text{h}/\text{AC}$ followed by $871^\circ\text{C}/20\text{h}/\text{AC}$.

Specimens for evaluating the defect-free SC's mechanical properties were machined from SC bars. The stress axis of the specimens was parallel to the growth direction of SC bars and was within 10° from the $\langle 100 \rangle$ direction. Specimens machined from DS slabs were used for evaluating mechanical properties of the SC with grain defects such as HAB. The stress axis of the specimens was the DS transverse direction which was perpendicular to grain boundaries. Bi-crystalline slabs were used for examining LAB strengths. The growth direction of both seeds was $\langle 001 \rangle$, which corresponded to the longitudinal direction of the slab. The primary seed was set in order to align the $\langle 110 \rangle$ direction parallel to the transverse direction of the slab. The $\langle 110 \rangle$ direction of the second seed was rotated from the transverse direction by α . Consequently, a grain boundary with a misorientation angle α was present along the center of the slab. Specimens were machined from the slabs parallel to the transverse direction. The grain boundary lay perpendicular to the stress axis in the middle of the specimen. The stress axis of the primary grain was parallel to the $\langle 110 \rangle$ direction, and the stress axis of the second grain deviated from the $\langle 110 \rangle$ direction by α in $\{100\}$ plane.

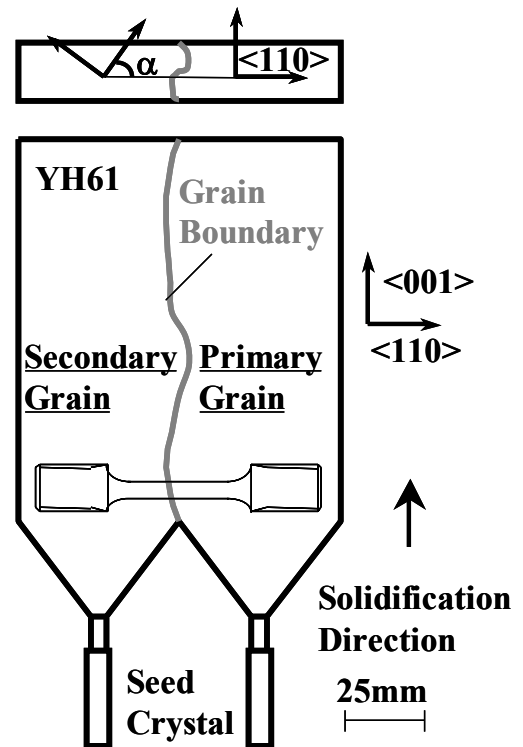


Fig. 1: Schematic of the bi-crystalline slab for evaluating the effect of α on strength of SC with LAB or HAB. Misorientation angle (α) was defined as rotation angle of the secondary grain against the primary grain on the $\{100\}$ plain.

Table 2 Solution Heat Treatment Conditions

Condition No.	Condition for Final Step
A	$1250^\circ\text{C}/4\text{h}/\text{AC}$
B	$1260^\circ\text{C}/4\text{h}/\text{AC}$
C	$1270^\circ\text{C}/4\text{h}/\text{AC}$
D	$1280^\circ\text{C}/4\text{h}/\text{AC}$
E	$1290^\circ\text{C}/4\text{h}/\text{AC}$
F	$1295^\circ\text{C}/4\text{h}/\text{AC}$

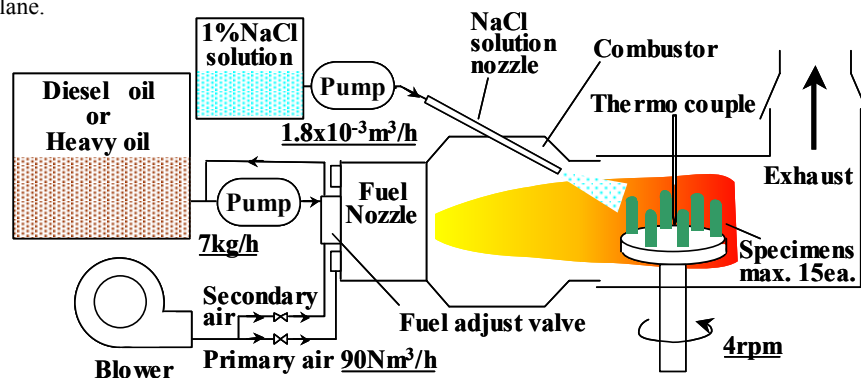


Fig. 2: A schematic view of the burner rig

Although IGTs' buckets and vanes are expected to contain a few grain boundaries and their solution heat treatment conditions should be determined with considering the possibility and degree of the actual boundaries, long-term creep strength of the alloy was evaluated by using specimens machined from defect-free SC castings heat-treated by the condition D. Creep tests for $\langle 110 \rangle$ direction as well as $\langle 100 \rangle$ were conducted to examine anisotropy of the alloy. The test temperature range studied was 750 to 1040°C and the stress range was determined to make the rupture lives about 100 to 10,000 hours. The maximum rupture life in this study was about 11,000 hours. General test conditions were based on ASTM E 139.

Hot corrosion resistance of the alloy was evaluated in a burner rig. Test specimens were machined from heat-treated SC castings containing no grain boundaries. Except for studying the effect of solution heat treatment condition on the hot corrosion resistance, the castings were heat-treated by the condition D which is the same condition as specimens for long-term creep data. Figure 2 shows a schematic view of the burner rig used in this study. The fuels used were diesel oil which contained about 0.04 mass% sulfur and heavy oil whose sulfur content was about 0.06 mass%. The diesel oil was used for the tests studying the effect of solution heat treatment condition on the hot corrosion resistance while the heavy oil was used for the other tests. 1 mass% NaCl solution was sprayed into the combustion gases at the rate of $1.8 \times 10^{-3} \text{ m}^3/\text{h}$. The test temperature was monitored at the center of the specimen holder. A single test cycle was 5 to 10 hours and the weight change of the specimens was measured after either one or two cycles. Before each measurement, the specimens were washed by hot water to remove combustion products other than the scale.

RESULTS AND DISCUSSION

The Effect of Solution Heat Treatment Conditions

The effect of solution heat treatment temperature on the volume percent of solutioned γ' is shown in Figure 3. The term "volume percent of solutioned γ' " is used to describe the volume percent of the region in which γ' is completely solutioned at the solution heat treatment and precipitated as fine particles during aging. The term or the vertical line in Figure 3 can be considered as describing how degree the specimen was solution-heat treated.

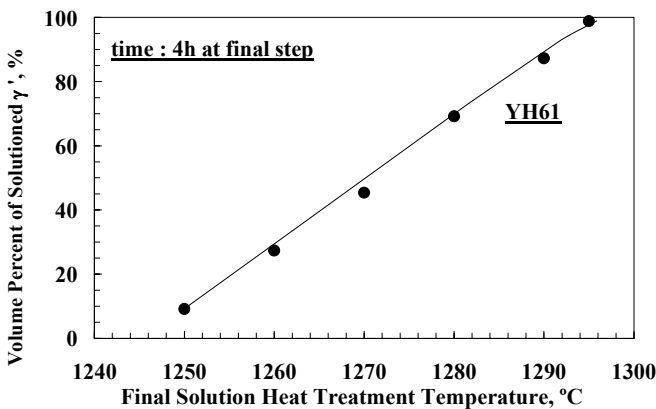


Fig. 3: Volume percent of solutioned γ' increased linearly with increasing solution heat treatment temperature in this temperature range.

A linear relationship between the volume percent of solutioned γ' and temperature was observed between 1250 and 1295°C. Although almost 100% solutioning with no incipient melting can be achieved in this alloy, residual eutectic γ - γ' colonies cannot be

dissolved without incipient melting due to its higher content of boron.

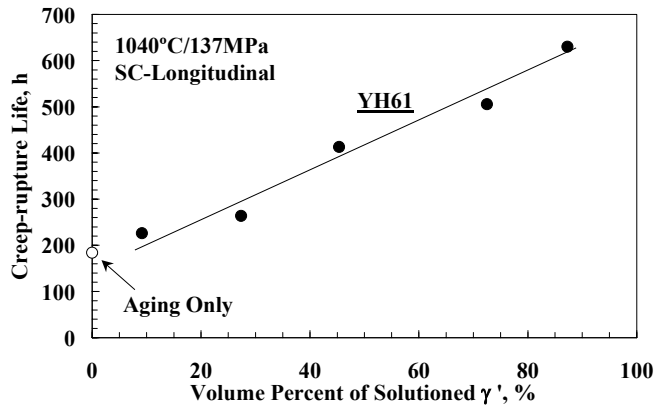


Fig. 4: Creep-rupture life of SC longitudinal direction increased with increasing volume percent of solutioned γ' .

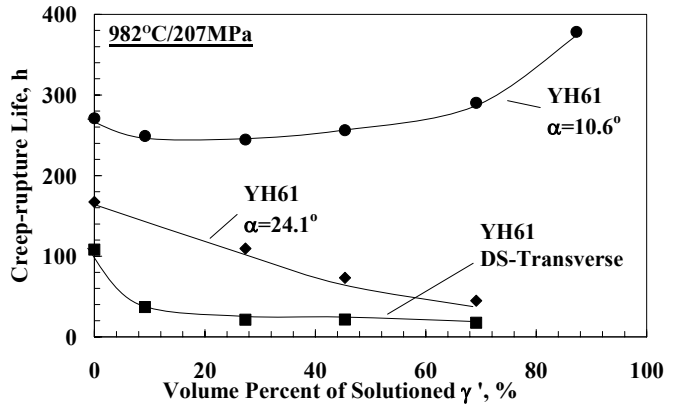


Fig. 5: The effects of solution heat treatment conditions on the creep-rupture life across the grain boundary depended on misorientation angle α .

The effect of solution heat treatment conditions on the creep-rupture life of defect-free SC longitudinal direction is shown in Figure 4. The creep-rupture life of the defect-free SC longitudinal direction was improved by increasing the volume percent of solutioned γ' . Although this result has already been established, it must be noted that the effects of solution heat treatment conditions on the creep-rupture life across the grain boundary showed different tendency as the defect-free SC longitudinal direction depending on misorientation angle α (Figure 5). When α was 24.1°, creep-rupture life across the grain boundary decreased with increasing the volume percent of solutioned γ' . It was opposite to that observed for the SC longitudinal direction but similar tendency as DS transverse direction. It was pointed out in our previous study (Tamaki et al., 1998) that the grain boundary surrounded by the non-solutioned γ' (Figure 6-a) still contains higher levels of boron after solution heat treatment. On the other hand, the grain boundary exposed to the solutioned γ' (Figure 6-b) was found to contain lower amounts of boron after solution heat treatment. If the solution heat treatment temperature or the treatment time is increased, the increase in the volume percent of solutioned γ' also increases the percentage of the exposed grain boundary. Thus, these could be considered as reasons why creep-rupture life for the higher α and DS transverse direction decreased with increasing the volume percent of solutioned γ' .

In case of $\alpha = 10.6^\circ$, no significant degradation of creep-rupture

life across the grain boundary was observed with increasing the volume percent. Additionally, a moderate fall-off of creep-rupture life was observed up to about 6° in SC610 which was full solutioned and did not contain boron (Figure 10). From these results, LAB might be defined as a grain boundary where creep-rupture life across the boundary does not show significant decrease with increasing the volume percent of solutioned γ' while the life across HAB significantly decreases with increasing the volume percent. It can be also deduced from these results that the presence of boron at grain boundaries does not play an important role in LAB while boron is essential for HAB strength. Therefore, it follows that the solution heat treatment condition would not influence the LAB strength significantly since diffusion of boron from the grain boundary during solution heat treatment is not a major issue for LAB strength. However, it must be noted that the addition of boron increases the misorientation angle at which there is a fall-off of strength, or rather, the addition of boron extends the range of LAB.

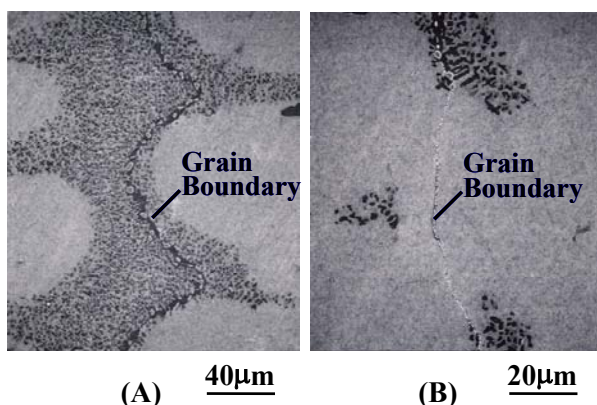


Fig. 6: Two typical grain boundary structures after solution heat treatment (Final step: 1290°C/4h).

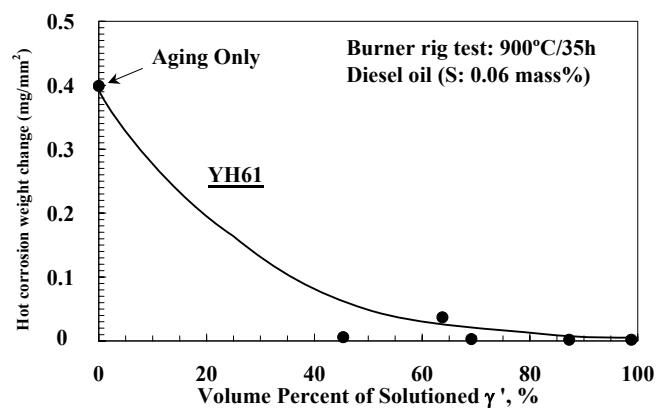


Fig. 7: Hot corrosion resistance of YH61 was improved by solution heat treatment.

Figure 7 describes the effect of solution heat treatment conditions on hot corrosion resistance of YH61. Hot corrosion resistance of YH61 was improved by increasing the volume percent of solutioned γ' or solution heat treatment temperature. Tamaki et al. (2002) found similar tendency in CM186LC which is one of the most popular second-generation DS alloys. Although decrease in element concentration inhomogeneity by solution heat treatment can be considered as one of the most possible reason why solution heat treatment improved hot corrosion resistance of the superalloy, they also pointed out that MC-type carbides acted as initiation sites for hot corrosion and the volume fraction of carbides decreased with increasing solution heat treatment time. Therefore, they

concluded that decreasing the volume fraction of carbides during solution heat treatment also could contribute to improving hot corrosion resistance of the alloy after solution heat treatment. In case of YH61, the similar mechanisms can be considered to improve hot corrosion resistance of the alloy.

The applicability of YH61 to IGTs

In order to confirm the applicability of YH61 to IGTs, long-term creep properties for both $\langle 100 \rangle$ and $\langle 110 \rangle$ direction, creep-rupture life of the specimens machined from SC buckets and vanes and hot corrosion resistance of the alloy were evaluated.

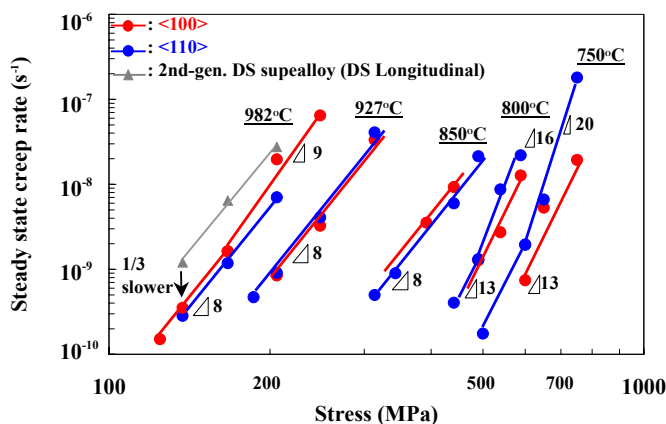


Fig. 8: The steady state creep rate is plotted as a function of the applied stress for $\langle 100 \rangle$ and $\langle 110 \rangle$ orientations of YH61. The slope of these lines indicates the stress exponent of the steady state creep rate, n for each temperature.

The creep-strengths of YH61 $\langle 100 \rangle$ and $\langle 110 \rangle$ orientations are represented by the relationship between steady state creep rate and applied stress for some temperatures (Figure 8). The steady state creep rates for both $\langle 100 \rangle$ and $\langle 110 \rangle$ orientations of YH61 were about one third as slow as that of a second-generation DS superalloy at 982 °C/137MPa. It should be noted that YH61 showed higher creep-strength than a second-generation DS alloy although Re content of YH61 is about half as much as that of second generation DS superalloys. Since Re is the most expensive element in Ni-based superalloys, it is very important to achieve higher creep-strength as low Re content as possible. It should be more emphasized in case of IGT components because their sizes are larger than those of the aero-engines'.

Figure 9 shows the effect of test temperature on the stress exponent of the steady state creep rates for YH61 $\langle 110 \rangle$ as well as $\langle 100 \rangle$ orientations. In general, the higher stress exponent indicates lower creep resistance. This result is supposed to mean that the creep resistance of $\langle 110 \rangle$ was lower than that of $\langle 100 \rangle$ at 800°C and below. On the other hand, when the test temperatures became higher than 800°C, the exponents for both $\langle 100 \rangle$ and $\langle 110 \rangle$ came to show almost same value and the creep rate for $\langle 110 \rangle$ was slightly slower than that of $\langle 100 \rangle$ at 982°C. It can be concluded from the above results that the anisotropy for creep strength between $\langle 100 \rangle$ and $\langle 110 \rangle$ should be major concern at 800°C and below while it was not significant at temperatures above 800°C. Although the creep strength of YH61 $\langle 110 \rangle$ direction was lower than that of the $\langle 100 \rangle$ direction especially at 750°C, other SC superalloys also show same tendency as reported by Wilcock et al. (2002). Shah and Duhl (1984) pointed out that tension yield strength of $\langle 110 \rangle$ is lower than that of $\langle 100 \rangle$ at 593°C for a SC superalloy PWA1480 although $\langle 110 \rangle$ and $\langle 100 \rangle$ orientations have the identical Schmid factor for the octahedral slip. It can be

deduced that this lower tension yield strength for $\langle 110 \rangle$ caused the lower creep resistance for $\langle 110 \rangle$ at temperatures below about 800°C. When the test temperature was higher than 800°C, other slip systems such as the cube slip can operate. Resultant isotropic deformation behavior can be considered to make the rate for $\langle 110 \rangle$ comparable to that for $\langle 100 \rangle$. The higher creep rate for $\langle 100 \rangle$ at higher stress of 982 °C might be caused by different rate of the rafting formation between $\langle 110 \rangle$ and $\langle 100 \rangle$.

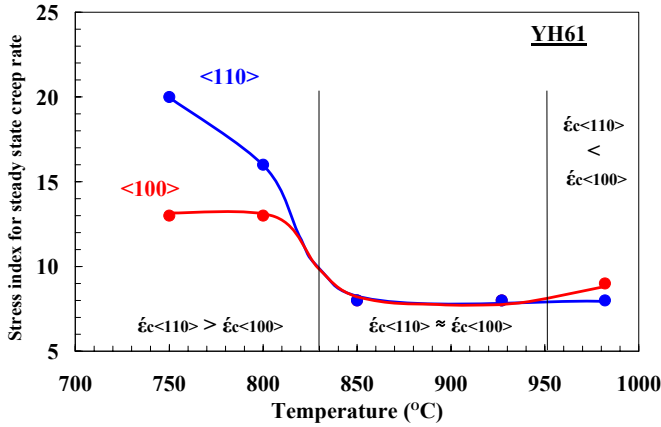


Fig. 9: The effect of test temperatures on the stress exponent of the steady state creep rates for YH61 $\langle 110 \rangle$ as well as $\langle 100 \rangle$ orientations

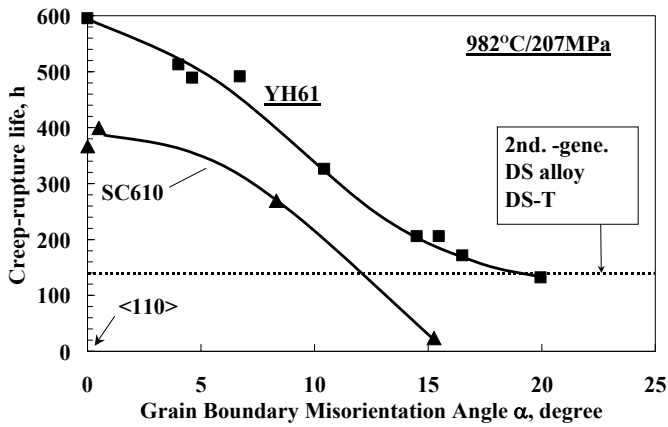


Fig. 10: The effect of grain boundary misorientation angle (α) on fall-off of creep-rupture life across LAB and HAB for YH61 compared with SC610

Figure 10 shows creep-rupture strength of YH61 across LAB and HAB compared with SC610 (Ni - 7.5Cr - 7.2W - 1.4Re - 0.8Mo - 8.8Ta - 1.7Nb - 5.0Al - 0.1Hf - 1.0Co, mass%, Sato et al., 1999) and creep-rupture strength of DS transverse direction for a second-generation DS superalloy. Although the creep-rupture strength of YH61 across grain boundary decreased with increasing α , it is higher than that of DS transverse strength when α was less than 20°. For comparison with SC610, the addition of boron and introducing the partial solution heat treatment to YH61 are supposed to cause higher HAB strength of YH61 than that of SC610 which contains no boron and is fully solution-heat-treated.

The casting trials for first stage buckets and vanes of a 25 MW class gas turbine were performed (Figure 11). Figure 12 shows creep-rupture life of the specimens machined from these buckets and vanes. No significant degradation was observed for the creep-rupture life of these specimens compared with that of specimens machined from SC bars ($\phi 15$ mm).



(a) Vane



(b) Bucket

Fig. 11: 25MW class IGT bucket and vane (first stage) made of YH61

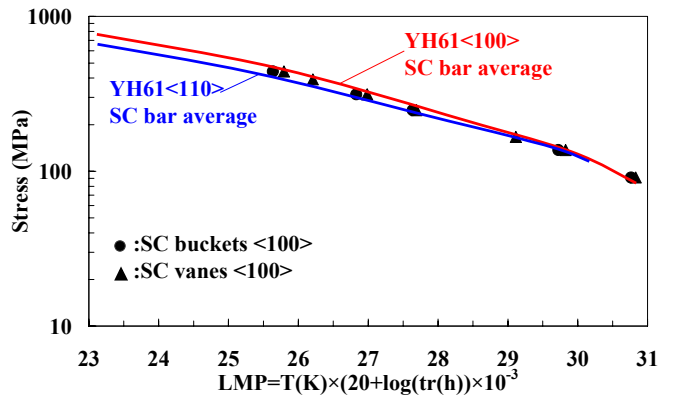


Fig. 12: Comparison of creep-rupture life indicated by using Larson-Millar parameter between the specimens machined from SC buckets, vanes and bars

Hot corrosion resistance of YH61 was evaluated by using the burner rig at 750, 900 and 1000 °C. The results are shown in Figure 13 with comparing with those of a second-generation DS superalloy and a 14% Cr containing CC superalloy. In the Figure, the vertical line indicates the time required to reach to 0.02 mg/mm² of hot corrosion weight change. Several points were extrapolated from the measured data. Hot corrosion resistance of YH61 was superior to that of a second-generation DS superalloy under the whole experimental temperature range and to that of a 14% Cr containing CC superalloy, which is currently used in some IGTs, when the test temperature was 1000°C. Figure 14 shows the secondary electron image and the corresponding characteristic

X-ray images (dot-maps) of the cross sectional view for YH61 after the burner rig test (900° C/60h). It is found that some dots for Cr agreed with dots for S near the front of corroded area. It can be concluded from the above result that Cr content of YH61 was enough to prevent S from forming low melting point eutectic with Ni after S penetrated underneath the oxide protective layer.

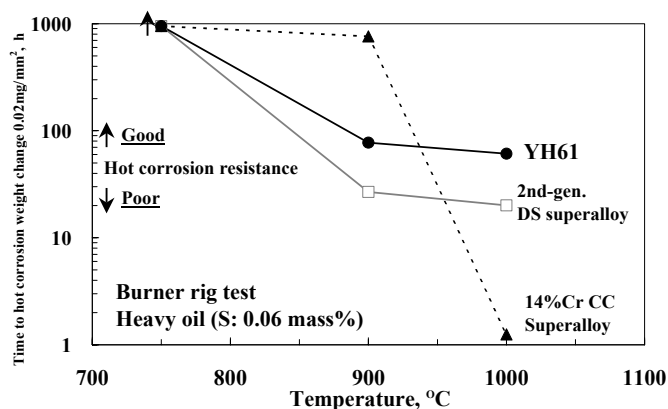


Fig. 13: The effect of test temperature on the hot corrosion resistance of YH61

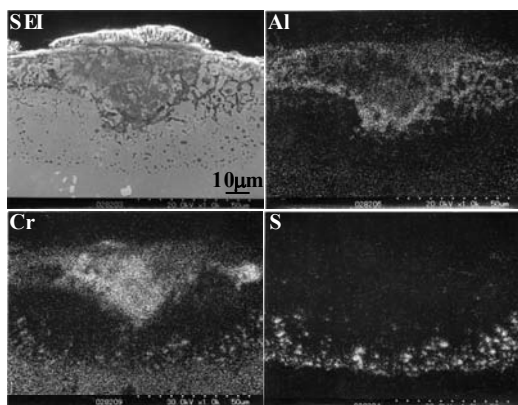


Fig. 14: A secondary electron image and corresponding characteristic X-ray images of corroded area in YH61 (after the test of 900° C/60h)

Conclusions

When SC castings are adopted for IGT's components, some degree of grain defects should be permitted to increase casting yield and reduce cost of the castings. In order to satisfy this demand, a new SC superalloy YH61 containing some grain boundary strengthening elements was developed. Although solution heat treatment has been known to improve mechanical properties of defect-free SC castings, it was found that solution heat treatment decreased mechanical properties of SC with grain defects. It should suggest that not only addition of grain boundary strengthening elements but also selecting proper solution heat treatment condition is important to permit some grain defects in SC castings. The solution heat treatment condition for YH61 was determined after considering compatibility for properties of both the defect-free SC and the SC with grain defects. The solution heat treatment was also found to improve hot corrosion resistance of the alloy.

In order to confirm the applicability of YH61 to IGTs, some properties, which are required to evaluate life of SC components,

were examined. YH61 showed higher creep strength than that of a second-generation DS superalloy although Re content of YH61 is about half as much as that of second-generation DS superalloys and also no significant degradation for creep-rupture life of the specimens machined from SC buckets and vanes was confirmed. Hot corrosion resistance of YH61 was superior to that of a second-generation DS superalloy under the whole experimental temperature range and to that of a 14% chromium containing CC superalloy, which is currently used in some IGTs, when the test temperature was 1000°C. Anisotropy for mechanical properties of SC should be considered to evaluate the SC components' life. In this alloy, it was found that the anisotropy for creep strength between <100> and <110> should be major concern at 800°C and below while it was not significant at temperatures above 800°C. The database for evaluating the life of SC components made of YH61 is mostly completed including the fatigue properties presented in another publication (Yorikawa et al., 2000).

REFERENCES

- Barker, T., 1995, "Siemens' New Generation", *Turbomachinery*, Jan/Feb, pp.20-22.
- Cetel, A.D. and Duhl, D.N., 1992, "Second Generation Columnar Grain Nickel-Based Superalloy", *Proceedings, Superalloys 1992*, S.D. Antolovich et al., ed., TMS, Warrendale, PA, pp.287-296.
- Cybulsky, M. and Bryant, P.E.C., 1993, "Application of Aero-Engine Turbine Materials Technology to Industrial Gas Turbines," *Advanced Materials and Coatings for Combustion Turbines*, V.P. Swaminathan and N.S. Cheruvu, ed., ASM, Materials Park, OH, pp.23-27.
- Farmer, R., 2002, "Reliant service-testing first 184-MW PG7251FB in simple cycle operation", *Gas Turbine World*, May/June, pp.10-14.
- Jackson, J.J. et al., 1977, "The Effect of Volume Percent of Fine γ' on Creep in DS Mar-M200 + Hf", *Metall. Trans. A*, Vol. 8A, pp.1615-1620.
- Kiesow, H.-J. and Mukherjee, D., 1997, "The GT24/GT26 Family Gas Turbine: Design for Manufacturing", *Advanced in Turbine Materials, Design and Manufacturing*, A. Strang et al., ed., The Institute of Materials, London, UK, pp.159-172.
- Ross, E.W. and O'Hara, K.S., 1996, "Renè N4: A First Generation Single Crystal Turbine Airfoil Alloy with Improved Oxidation Resistance, Low Angle Grain Boundary Strength and Superior Long Time Rupture Strength", *Proceedings, Superalloys 1996*, R.D. Kissinger et al., ed., TMS, Warrendale, PA, pp.19-25.
- Sato, K., Tamaki, H. et al., 1999, "High Corrosion Resistant High Strength Superalloy and Gas Turbine Utilizing The Alloy", U.S. Patent 5,916,382.
- Shah, D.M. and Duhl, D.N., 1984, "The Effect of Orientation, Temperature and Gamma Prime Size on the Yield Strength of a Single Crystal Nickel Base Superalloy", *Proceedings, Superalloys 1984*, M. Gell et al., ed., TMS, Warrendale, PA, pp.105-114.
- Tamaki, H. et al., 1998, "Development of A New Ni-Based Single Crystal Superalloy for Large Sized Buckets", *Materials for Advanced Power Engineering 1998*, J. Lecomte-Beckers et al., ed., Forschungszentrum Jülich GmbH, Jülich, Germany, pp.1099-1110.
- Tamaki, H. et al., 2000, "Development of A Low Angle Grain Boundary Resistant Single Crystal Superalloys YH61", *Proceedings, Superalloys 2000*, T.M. Pollock et al., ed., TMS, Warrendale, PA, pp.757-766.
- Tamaki, H. et al., 2002, "Effect of Solution Heat Treatment of The Hot Corrosion Resistance of A Second Generation DS Superalloy", *Materials for Advanced Power Engineering*

2002, J. Lecomte-Beckers et al., ed., Forschungszentrum Jülich GmbH, Jülich, Germany, pp.355-364.

Yorikawa, M. et al., 2000, "Thermal Fatigue Crack Initiation and Growth Behavior under FCI Condition in Cylindrical Specimen of Ni Base Superalloys", *Proceedings, The 40th Symposium on Strength of Materials at High Temperatures* The Society of Materials Science, Kyoto, Japan, pp.31-35.

Wilcock, I.M. et al., 2002, "The Creep Behavior of As-Cast SX CM186LC at Industrial Gas Turbine Operating Conditions", *Materials for Advanced Power Engineering 2002*, J. Lecomte-Beckers et al., ed., Forschungszentrum Jülich GmbH, Jülich, Germany, pp.139-148.

